UNBONDED PRESTRESSED COLUMNS FOR EARTHQUAKE RESISTANCE

Alex S. Larkin[1], David H. Sanders[2], M. Saiid Saiidi[3]

Abstract

The implementation of unbonded post-tensioning in bridge columns reduces damage and repair time by minimizing residual displacements. This research investigates the use of unbonded post-tensioned tendons in bridge columns. Two unbonded post-tensioned columns were tested that are identical except for the amount of longitudinal reinforcement crossing the joint between the footing and column base. The placement of post-tensioning in a full-scale column was taken into consideration which resulted in four tendons being placed around the center of the column cross section instead of one through the center of the column as has been done in previous experiments. The tendons are anchored in the side of the footing for ease of replacement following an earthquake.

Introduction

The number one concern for engineering seismic design is to maintain life safety. Once a structure can maintain life safety through an earthquake, the next step is to minimize the amount of damage to the affected structure. Minimizing the amount of damage will allow for rapid repairs and minimal closure time. For bridge columns, the use of unbonded post-tensioned tendons reduces the amount of residual displacement following an earthquake, allowing for minimal closure time of the bridge while repairs are made.

For full-scale columns, the amount of post-tensioning needed to promote re-centering effects would be between 8% and 10% $f'_c A_g$. Typically, the initial stress in the tendons is between 20% to 30% f_{pu}. Therefore, if the column is 60 inches (1524 mm) in diameter, and 0.6 in (15.2 mm) strands are used, a total of between 62 and 86 strands would be needed. In addition to this being a large number for one tendon, multiple tendons allows for a tendon to be replaced while still maintaining post-tensioning and also increases redundancy. The columns being tested are 0.4-scale model, with a diameter of 24 in (610 mm). Therefore, to evenly distribute the force required for re-centering, four tendons, each with four 0.6 in (15.2 mm) Grade 270 ksi

[1]Graduate Research Assistant, University of Nevada Reno
[2]Professor, University of Nevada Reno
[3]Professor, University of Nevada Reno

(1862 MPa) 7-wire strands were evenly spaced at 5.4 in. (137.2 mm) around the center of the column cross section (see Fig. 1).

Following a major earthquake, bridge columns are likely to have undergone large lateral displacements. Post-tensioned columns are typically designed to not have tendons yield or be damaged. It is critical for it to be possible to inspect and replace the tendons. Previous tests have utilized straight tendon or bar that exited through the bottom of the footing; this configuration makes it impossible to replace the tendon. By exiting out the side, or out the top of the footing for large footings (180 degree bend for the post-tensioning tendon), the tendons can be removed. For these specimens, the tendons exited out the side of the footing (see Fig. 2).

Literature Review

Excessive residual displacement is an issue with columns following an earthquake. Unbonded post-tensioned tendons have been used in columns that have shown reductions in residual displacements. Research performed by Ou showed the re-centering capabilities of unbonded post-tensioned columns. Ou's report also indicates that high lateral column displacements lead to high strain in the unbonded post-tensioned tendons (Ou et. al. 2009). Hewes has also indicated the importance in the selection of the initial post-tensioned force in the tendon. The higher tendon forces aid in reducing the residual displacements at low drift levels, but can lose their effectiveness at high drift ratios due to the yielding of the tendon. Hewes' report also indicates the benefit of using unbonded tendons as opposed to bonded tendons because the localized inelastic straining due to large drifts can be avoided, maintaining the re-centering force throughout testing or throughout an actual earthquake (Hewes and Priestley 2002). While the column may still show damage depending on the intensity of the earthquake, repairs can be made quicker when the column re-centers itself. Sakai concluded that adding a steel jacket to the column plastic hinge region as well as locally unbonding the mild reinforcing steel that cross the joint between the footing and column base prevented damage compared to a conventionally reinforced column and a partially prestressed column (Sakai et. al.2006).

Justification

The amount of post-tensioning was selected by keeping the initial force (10% f'_cA_g) in the post-tensioning at or below a tendon stress of 20% f_{pu}. The amount of longitudinal reinforcement that crosses the joint between the footing and the base of the column was selected based on the literature review. Much of the previous post-tensioning experiments had very little to no longitudinal reinforcement crossing the

joint between the footing and column as past researchers were just interested in the re-centering effects of the tendon. Now that post-tensioning has shown excellent re-centering effects, the combination of post-tensioning with longitudinal reinforcement should be investigated. Sakai had a longitudinal reinforcement ratio of 0.65% with a single tendon in his report. This amount of reinforcement allows for some longitudinal column capacity in case of a tendon failure, and is small enough to allow for minimal residual displacement. While the research described in this paper utilized several tendons located around the center of the column cross section, it used a small longitudinal reinforcement ratio to capture the re-centering effects for one column. The second columns reinforcement ratio was doubled from the first to determine how the amount of longitudinal reinforcement affects re-centering.

Design of Specimens and Test Setup

The two columns selected for testing were initially targeted to have identical properties except for the amount of longitudinal reinforcement crossing the joint between the footing and the column base. Achieving identical forces in the tendons between the two columns was difficult and ended with slight variations in the initial post-tensioning ($\%f'_cA_g$) between the two specimens. The column parameters are shown in Table 1 and the cross section for each column is shown in Figure 1. The material properties for each column are shown in Tables 2 and 3.

The test setup for each column consisted of a reaction wall, strong floor, and a 220-kip actuator to produce the cyclic loading protocol in Figure 3. The reaction wall was created by stacking two columns of three 4x4x8 foot (1.22x1.22x2.44 m) concrete blocks, with one additional block added to the top of the front stack to achieve the proper height for the actuator to meet the column head. The reaction wall was secured to the strong floor using 1.25 in. (31.75 mm) Dywidag™ post-tensioned bars. The footing of each column was secured to the 3 foot (0.91 m) deep strong floor with six 1.25 in. (31.75 mm) Dywidag™ post-tensioned bars. Each Dywidag™ bar for the reaction wall and footing had a 100 kip (444.84 kN) force applied.

A steel spreader beam was bolted to the top of the column to apply the axial dead load. Two hydraulic rams were attached to the top of the spreader beam on each side of the column and two high strength 1.25 in. (31.75 mm) threaded rods ran through the hydraulic ram, load cell, footing, and attached to the bottom of the strong floor to apply the axial dead load. The axial dead load was maintained through an accumulator which held constant and equal load in each of the hydraulic rams throughout testing. The test setup is shown in Figure 4.

Results

The cyclic loading for each column produced a lateral force and displacement hysteresis curve. The hysteresis curve was broken up into the positive backbone envelope, considered the push cycle, and the negative backbone envelope, considered the pull cycle. The absolute values from the negative backbone envelope were superimposed with the positive backbone envelope and an average curve was taken from the two envelopes. The average curve is considered the pushover curve for the column. The pushover curve for columns PT-LL and PT-HL are shown in Figures 5 and 6 respectively.

Column PT-LL had a first bar yield displacement of 0.63 in (16.0 mm). This was determined by finding the displacement when the first longitudinal bar yielded. This value was used to plot a straight line on the pushover curve, beginning at zero displacement and zero force. A straight line was then plotted across the top of the curve, where the area under the straight line bounded by the top of the pushover curve was equal to the area under the pushover curve bounded by the straight line. The point at which these two straight lines intersect is the effective yield displacement (0.95 in. (24.2 mm). The ultimate displacement was defined as the displacement at 80% of the peak lateral force in the column. The ultimate displacement of column PT-LL was 8.64 in (219.5 mm) at a drift of 8.0%, and a displacement ductility of 9.1. Column PT-HL had a first yield displacement of 1.0 in (25.4 mm) that lead to an effective yield displacement of 1.36 in (34.5 mm). The ultimate displacement for column PT-HL was 9.17 in (232.9 mm) at a drift of 8.5% resulting in a displacement ductility of 6.7.

Each of the four tendons consisted of four 0.6” (15.24 mm) Grade 270 ksi (1862 MPa) 7-wire strands. Tendons 2 and 4 were located on the same axis that the column was rotated about. Tendons 1 and 3 were located on the extreme ends and felt the largest strains. The initial force in the tendons was carefully selected and kept within the lower elastic region so the tendons would not yield under large lateral displacements. Figures 7 and 8 show the microstrain in tendons 1 and 4 with respect to the drift ratio of the column. The outermost tendons (tendons 1 and 3) felt the largest strains as shown in Figure 7, compared with tendons located on the same axis the columns were rotated about (tendons 2 and 4) shown in Figure 8. The tendons do not begin to yield until a microstrain of at least 8000 is reached. It can be seen that even the most extreme tendons, such as tendon 1 did not reach their yield strains, even at very large drift ratios. Column PT-HL behaved very similarly to column PT-LL and did not reach a strain of more than 6500 microstrains, even at drift levels as high as 10%.

Figure 9 shows the full hysteresis curve for column PT-LL. During construction, the cover concrete was almost double the amount on one side of the column in relation to the other side. Uneven column cover lead to the core being shifted and not in the true center, causing residual displacements and peak loads to differ from a push and pull cycle. Figure 9 displays the enhanced re-centering effect provided by post-tensioning. At a drift level of 6% (6.48 in, 164.6 mm), column PT-LL had a residual displacement on the positive side of the hysteresis curve of 1.57 in (39.9 mm) and a residual displacement on the negative side of the hysteresis curve of 3.45 in (87.6 mm), resulting in an average residual displacement of 2.51 in (63.8 mm). The full hysteresis for column PT-HL is shown in Figure 10. The residual displacements are larger than PT-LL due to the increase in amount of longitudinal reinforcement. At a drift level of 6% (6.48 in, 164.6 mm), column PT-HL had a residual displacement on the positive side of the hysteresis curve of 3.12 in (79.2 mm) and a residual displacement on the negative side of the hysteresis curve of 3.31 in (84.1 mm), resulting in an average residual displacement of 3.22 in (81.7 mm).

Conclusions

Two unbonded post-tensioned columns have been tested for seismic design. The columns had identical properties except for the amount of longitudinal reinforcement crossing the joint between the footing and the base of the column. Each column had four tendons evenly spaced around the center of the column cross section to evenly distribute the force required for re-centering. While past research has anchored the tendons in the base of the footing, this research anchored the tendons in the side of the footing for the ease of inspection and replacement following an earthquake.

Tendon location and the initial tendon force selected (based on keeping the post-tensioning at or below an initial tendon stress of 20% f_{pu}) were satisfactory. The extreme tendons (tendons 1 and 3) did not begin to yield, even at large drift ratios of 10% (10.8 in, 274.3 mm). Tendons located at 22.5% of the column diameter from the center of the column cross section provide re-centering capabilities and do not yield at large drift ratios. Exiting the tendons out the side of the footing did not display any negative effects.

The amount of longitudinal reinforcement had a large impact on the re-centering capabilities of the column. PT-LL had a residual displacement of 1.5 in (38.1 mm) at 6% drift (6.48 in, 164.6 mm), while column PT-HL had a residual displacement of 3.1 in (78.7 mm) at 6% drift (6.48 in, 164.6 mm. The displacement ductility of column PT-LL was 8.1 as opposed to 6.7 for column PT-HL.

Acknowledgments

Support for this research was provided by the Nevada Department of Transportation. The findings herein are of the authors and do not necessarily represent those of the sponsoring organization

Conversions

US Customery Units	SI Equivalent
1 in	25.4 mm
1 ft	0.3048 m
1 kip	4.45 kN

.

References

Hewes, J. T., and Priestley, M. J. N. (2002). "Seismic Design and Performance of Precast Concrete Segmental Bridge Columns." Structural Systems Research Project, *Rep. No. SSRP-2001/25*, University of California, San Diego, La Jolla, California.

Ou, Y., Wang, P.-H., Tsai, M.-C., Chang, K.-C., and Lee, G. C. (2009). "Large-scale experimental study of precast segmental unbonded post-tensioned concrete bridge columns for seismic regions." *Journal of Structural Engineering, ASCE*

Sakai, J., H. Jeong and S. Mahin, "Reinforced Concrete Bridge Columns that Re-Center Following Earthquakes," *Proceeding, 8th national Conference on Earthquake Engineering, EERI,* San Francisco, CA, April 2006, Paper 1421.

TABLE 1: COLUMN PARAMETERS

Column	ρ_l	ρ_s	PT (initial)	Dead Load	Height, in (m)	Diameter, in (m)	Aspect Ratio
PT-LL	0.685% (10 #5's)	1.00%	8%f'cAg, 157 kips (698 kN)	6%f'cAg (122 kips)	108 (2.74)	24 (0.61)	4.5
PT-HL	1.33% (10 #'7's)	1.00%	9%f'cAg, 186 kips (827 kN)	6%f'cAg (122 kips)	108 (2.74)	24 (0.61)	4.5

TABLE 2: CONCRETE PROPERTIES

Column	Segment	7-Day Strength, psi (MPa)	Test Day, psi (MPa)
PT-LL	Footing	4361 (30.1)	5384 (37.1)
	Column & Column Head	3380 (23.3)	4330 (29.9)
PT-HL	Footing	4361 (30.1)	5500 (37.9)
	Column & Column Head	3380 (23.3)	4570 (31.5)

TABLE 3: STEEL PROPERTIES FOR COLUMN PT-LL

Tested Bar	f_y, psi (MPa)	f_u, psi (MPa)
Transverse Bars: #3	71300 (492)	94500 (652)
Longitudinal Bars: #5	71800 (495)	96600 (666)
Longitudinal Bars: #7	69800 (481)	112200 (774)
Post-tensioned Strand: 0.6"	247000 (1703)	281000 (1937)

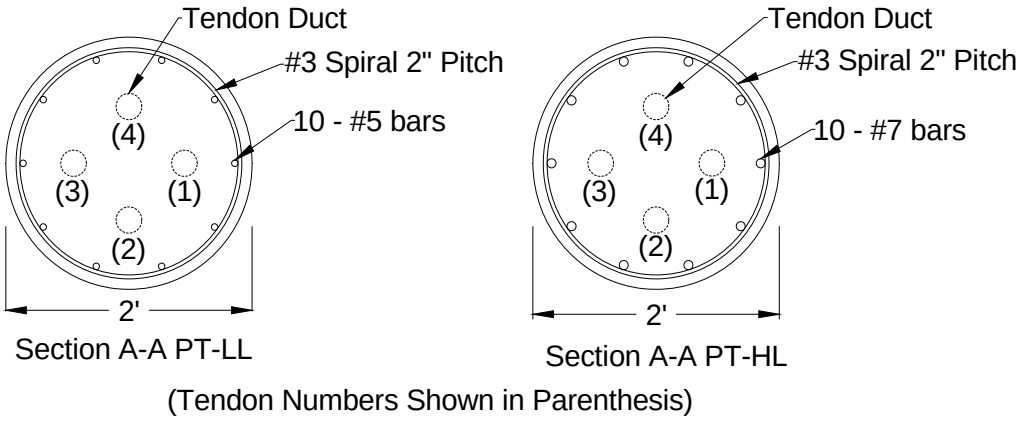

FIGURE 1: CROSS SECTION FOR PT-LL AND PT-HL

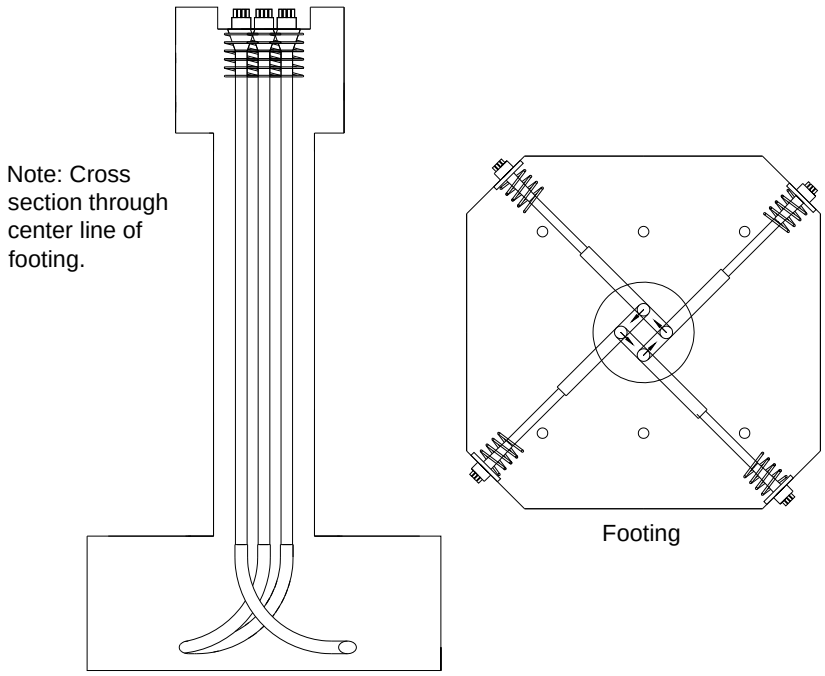

FIGURE 2: TENDONS EXITING OUT THE SIDE OF THE FOOTING

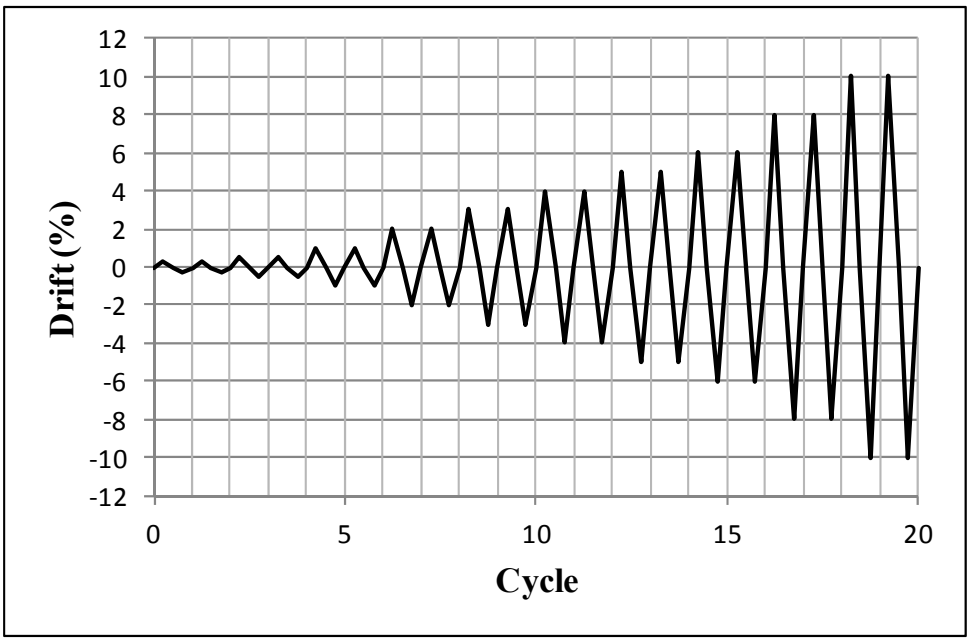

FIGURE 3: LOADING PROTOCOL

FIGURE 4: TEST SETUP

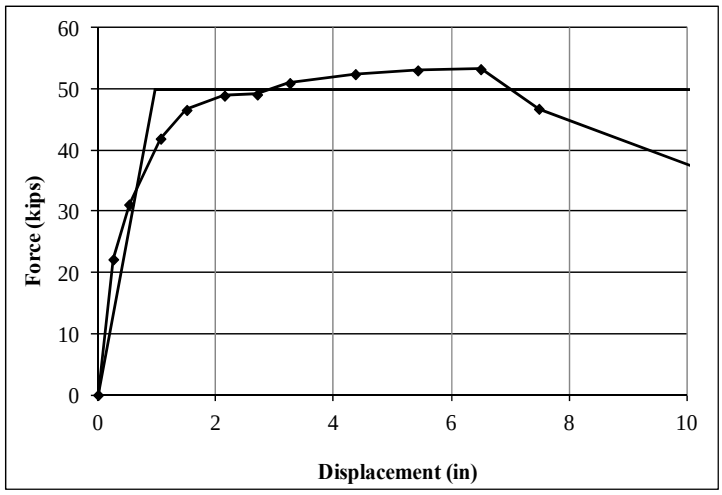

FIGURE 5: AVERAGE PUSHOVER PT-LL

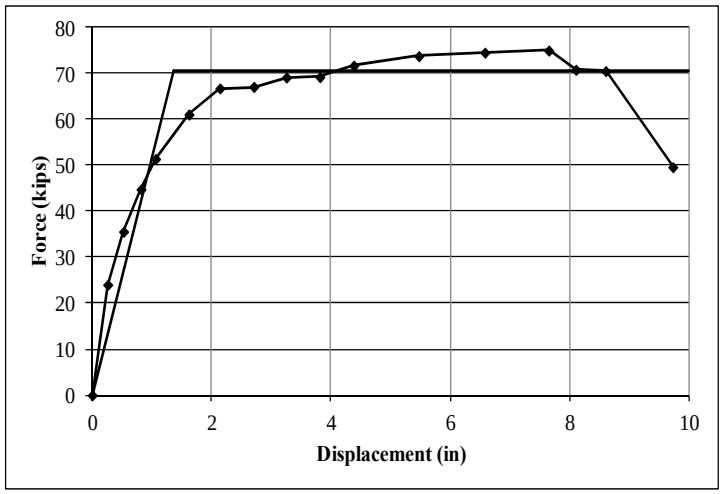

FIGURE 6: AVERAGE PUSHOVER PT-HL

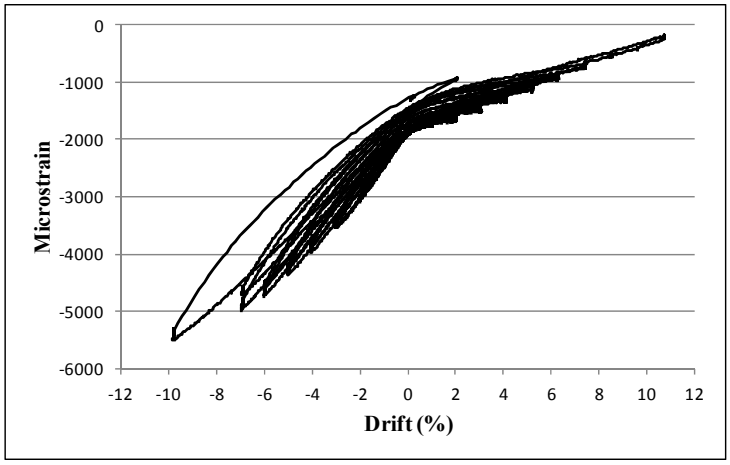

FIGURE 7: STRAIN IN TENDON 1 PT-LL

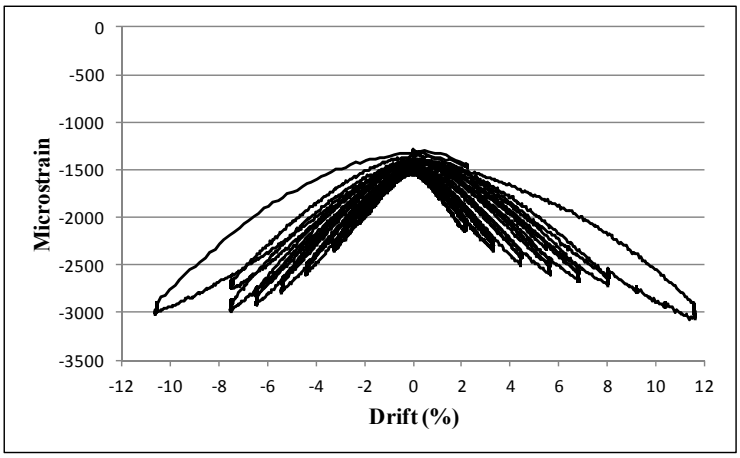

FIGURE 8: STRAIN IN TENDON 4 PT-LL

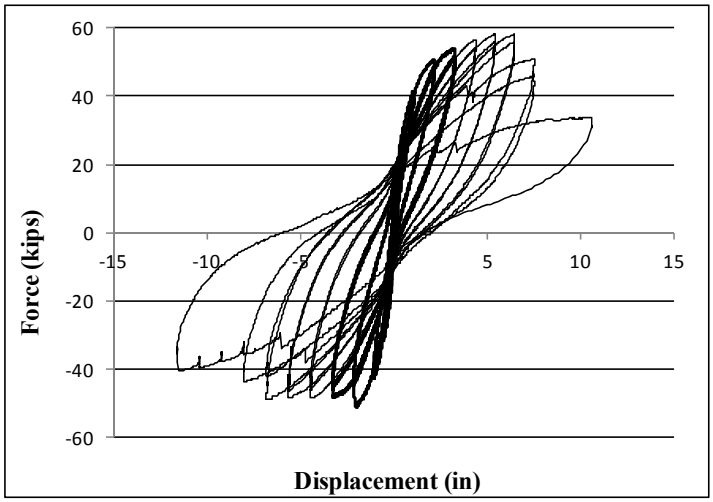

FIGURE 9: HYSTERESIS PT-LL

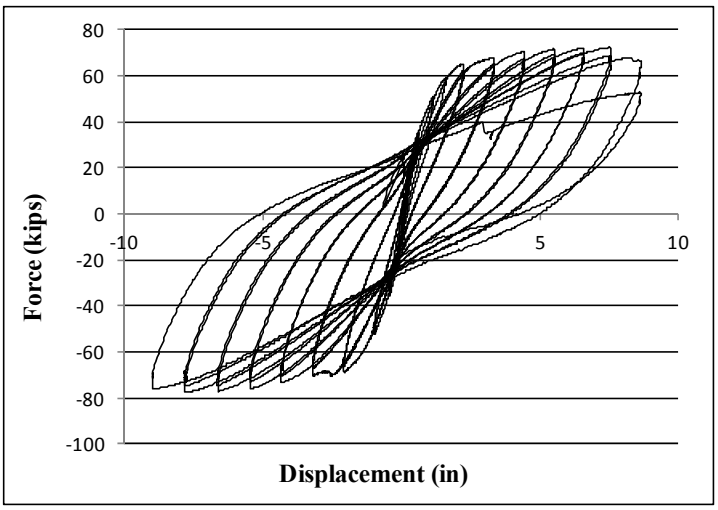

FIGURE 10: HYSTERESIS PT-HL